(22) Hamburg, A. W.; Nemeth, M. T.; Margerum, D. W. *Inorg. Chem.* **1983**, *22*, 3535.
(23) Michielin, L.; Mammi, S.; Peggion, E. *Biopolymers* **1983**, *22*, 2325.
(24) *Handbook of Biochemistry and Molecular Biology*, 3rd ed.; Fasman, G. D., Ed.; CRC Press, Inc.: Boca Raton, FL, 1975; Vol. I, p 121.
(25) Kaneko, M.; Tsuchida, E. *Macromol. Rev.* **1981**, *16*, 397.

Structure and Morphology of Ethylene–Vinyl Chloride Copolymers

M. A. Gomez,† A. E. Tonelli,* A. J. Lovinger, F. C. Schilling, M. H. Cozine,‡ and D. D. Davis

AT&T Bell Laboratories, Murray Hill, New Jersey 07974. *Received October 27, 1988; Revised Manuscript Received May 2, 1989*

ABSTRACT: A series of ethylene–vinyl chloride copolymers with a sequence distribution toward the alternating side of random and a wide range of comonomer content (up to 37.3 mol % vinyl chloride) have been examined in the solid state by diffraction and microscopic techniques and high-resolution ^{13}C NMR spectroscopy. Significant expansion of the unit cell in the *a* dimension, observed as the amount of chlorine in the copolymer increases, indicates a significant incorporation of the Cl substituents inside the crystal. X-ray diffraction also shows progressive intermolecular disorder with increasing vinyl chloride content, resulting in a change in the packing of chains from orthorhombic to pseudohexagonal. Differences in the chemical shifts of crystalline and amorphous CH(Cl) resonances, together with differences in their mobilities (T_1's) as observed by solid-state ^{13}C NMR spectroscopy, cooroborate the incorporation of Cl inside the crystal. Comparison of quantitative ^{13}C NMR spectra at temperatures above and below the melting point indicates that at least 20% of the Cl's reside inside the crystal. The irregular distribution of chlorine in our copolymers also affects their morphology. Electron microscopy showed the lamellar characteristics to progressively depart from those of polyethylene, although the preferred growth direction and the molecular chain axis tilt within the crystals are preserved for the copolymers with up to 2.4 mol % Cl content. For higher Cl contents, the crystals become increasingly more disordered and defective but retain an essentially lamellar character for copolymers with up to 21.2 mol % Cl.

Introduction

One of the most important and controversial aspects in the study of copolymer crystallization is the incorporation of branches or sidechains into the crystal. A large body of work has been devoted to this topic, especially for ethylene copolymers.[1-10] While some theories[1,11] consider the side chains and branches to be totally excluded from the crystals during the crystallization process, experimental results seem to indicate that they are at least partially incorporated in some cases.[2-5] In their kinetic theory of copolymer crystallization, Helfand and Lauritzen[7] have removed the assumption that only one of the two comonomer units constituting a copolymer is permitted to enter the crystal. They found that the composition of comonomer units in the crystal increasingly departs from their equilibrium composition as the rate of crystallization is increased by lowering the crystallization temperature. We will discuss their result in relation to the observations made here on crystalline ethylene–vinyl chloride copolymers.

In the case of ethylene copolymers, it seems to be generally accepted that methyl groups are easily incorporated into the crystal,[3,8,12,13] but there are different points of view in relation to other longer and bulkier branches.[3,5,12] Experimentally, the expansion of the unit cell as determined by X-ray diffraction has been considered as proof of the incorporation of the branches, although it has been pointed out that other factors can also account for this expansion.[12,14] The extent to which the branches are accommodated has been reported to depend upon the side-chain length and crystallization conditions. Baker and Mandelkern[3] studied several ethylene copolymers and found that methyl groups expand the crystal lattice while larger branches do not. However, other workers[2,5,15] concluded that longer branches, up to ten carbons in length, could be incorporated in the crystal lattice as evidenced by X-ray diffraction.

Supporting experimental evidence comes from the dependence of the melting behavior of copolymers on their comonomer composition. It has been concluded that methyl groups not only enter the crystal lattice in a significant proportion, but they do so as part of an equilibrium process,[12,13] resulting in significantly higher melting temperatures than ethylene copolymers with longer alkyl-type side chains. Branches larger than methyl groups were found[12] to be excluded from the crystal and their melting behavior to be very dependent on overall comonomer concentration and distribution but independent of the chemical nature of the side chain.[12]

Apparently many factors affect the incorporation of these branches into the crystalline lattice. However, even more important is the establishment of their distribution between amorphous, interfacial, and crystalline phases and the characterization of the degree of disorder introduced into the crystal by their incorporation. Several studies have dealt with this topic employing mainly small-angle X-ray and neutron scattering[9,16,17] and recently solid-state ^{13}C NMR.[18-21]

In previous work,[22-24] we have studied and characterized by different techniques a series of ethylene–vinyl chloride (E–V) copolymers. These copolymers were obtained by reductive dechlorination of poly(vinyl chloride), and they have a "random"-like comonomer sequence distribution. Because they are all obtained from the same parent compound, each copolymer is of the same average chain length and polydispersity; the major distinguishing characteristic among them is their chlorine content. Moreover, the van

† Permanent address: Instituto de Ciencia y Tecnología de Polimeros, Juan de la Cierva 3, 28006 Madrid, Spain. Work done while at AT&T Bell Labs.
‡ Permanent address: Department of Chemistry, Yale University, New Haven, Connecticut. Work done while at AT&T Bell Labs.

0024-9297/89/2222-4441$01.50/0

Table I
Characteristics of the E–V Copolymer Samples

polymer	Cl/100 C	T_g, °C	T_m, °C
PE			128
EV-2.4	1.2		112
EV-13.6	6.8		78
EV-21.2	10.6	−43	54
EV-37.3	18.6	−26.5	20

der Waals radius of Cl is similar to the effective radius of the methyl group. Consequently, these copolymers are ideal materials for studying the incorporation of methyl-type side chains into the crystal without complications arising from other structural differences.

Solid-state ^{13}C NMR is a very useful technique for discriminating between solid phases and not only provides conformational information about each phase but also detects differences in molecular mobility between the phases.[25] The NMR motional parameters are expected to be very sensitive, for example, to the presence of defects inside the crystal.

Here we describe a study of the effect of increasing chlorine content on the structure and morphology of a series of ethylene–vinyl chloride (E–V) copolymers and on some of their related properties such as crystallinity and effective crystallite size. X-ray, electron diffraction, and electron microscopic techniques have been combined with solid-state ^{13}C NMR to characterize the structural aspects of these E–V copolymers. The degree of incorporation of chlorine inside the copolymer crystals has been examined together with the effects of different crystallization conditions.

Experimental Section

The E–V copolymers studied here were prepared by the reductive dechlorination of poly(vinyl chloride) (PVC) (Aldrich no. 18958-8) with tri-*n*-butyltin hydride [$(n\text{-Bu})_3$SnH], as described elsewhere.[22,23] The complete range of comonomer composition was obtained from PVC to polyethylene (PE). The present study only deals with those E–V copolymers that are semicrystalline, as previously determined by DSC[22] (less than 40 mol % V units). Table I summarizes the most important characteristics of the E–V copolymers, their compositions, and abbreviations. For example, E-V-13.6 refers to an E–V copolymer with 13.6 mol % of V (vinyl chloride) units. Analysis of the ^{13}C NMR spectra recorded for the copolymer solutions was used to determine their comonomer composition and sequence distributions, and it was established that each E–V copolymer has a nearly "random" comonomer sequence.[23]

Actually, the comonomer sequences in E–V copolymers produced by $(n\text{-Bu})_3$SnH reduction of PVC were found to be on the alternating side of truly random rather than blocky. This is a consequence of the preference by $(n\text{-Bu})_3$SnH to remove Cl atoms from V* units surrounded by other V units (···VV*V···) compared with the removal of Cl from an isolated V* unit (···EV*E···). Study[26,27] of the $(n\text{-Bu})_3$SnH reduction of the PVC model compounds 2,4-dichloropentane and 2,4,6-trichloroheptane led to quantitative estimates for this preference and permitted the complete reduction of PVC by $(n\text{-Bu})_3$SnH to be simulated by computer. This simulation enabled us to determine comonomer sequences of any length in the E–V copolymers, not just to the comonomer triad level as permitted by analysis[23] of their ^{13}C NMR solution spectra.

In addition, the PVC from which all the copolymers were obtained is known to have 1–3 branches[28] per 1000 backbone carbon atoms and a measured molecular weight,[23] M_n = 58 000.

The principal advantage of these E–V copolymers is that the only variable across their range of composition is the chlorine content and sequence. Each copolymer has the same degree of polymerization (ca. 1000) and the same long-chain branching structure. Thus, we can observe the effects of chlorine content in the absence of other structural variations. In addition, all copolymer results are compared with the observations made for the PE obtained by the complete reductive dechlorination of the same PVC.

Two different crystallization conditions were employed in all of the experiments. Each E–V sample was (a) quenched rapidly from the melt to room temperature and (b) isothermally crystallized over night from the melt at temperatures 10–25 °C below the melting point and then quenched to room temperature.

X-ray diffractograms were recorded in the reflection geometry on a Rigaku diffractometer at 1° (2θ)/min under Ni-filtered Cu Kα radiation. Fiber patterns of oriented specimens were recorded on flat film in a vacuum camera.

The fusion and crystallization of the E–V samples under different conditions were monitored by calorimetry. A Perkin-Elmer DSC-4 instrument was used with a heating rate of 10 °C/min. Melting points were identified with the maximum in the endothermic peak.[29] The enthalpies of fusion determined from the DSC thermograms were converted to degrees of crystallinity by comparison to the enthalpy of fusion ΔH_u of a perfect PE crystal at the melting point of the copolymer.[12] ΔH_u at T_m was taken[30] to be 69 cal/g and ΔC_p = 0.0713 cal/(°C·g).

^{13}C NMR measurements in the solid state were carried out on a Varian XL-200 spectrometer operating at a static field of 4.7 T. Variable-temperature, magic angle sample spinning (MAS) was achieved with a Doty Scientific probe that utilizes a double air bearing design. All the samples were spun at speeds of ca. 3 kHz in aluminum oxide rotors with Kel-F [poly(chlorotrifluoroethylene)] end caps. A 45-kHz rf field strength was used for the dipolar decoupling (DD) of proton spins, with a decoupling period of 200 ms.

The usual cross-polarization (CP) sequence with optimum contact time of 1000 μs was employed. The spectra without CP were recorded with different waiting times after the acquisition of an FID to obtain spectra containing partial or total contributions from the amorphous and crystalline components of our samples. Spin–lattice relaxation times, T_1, longer than a few seconds were measured by the pulse sequence with CP developed by Torchia[31] while the shorter T_1's were obtained by the standard saturation–recovery pulse sequence[32] without CP. All spectra were referenced to the resonance of poly(oxymethylene) (POM) (89.1 ppm from TMS).[33]

Ultrathin copolymer films cast from solution, as well as polymer single crystals also grown from dilute solution, were prepared for electron microscopy and diffraction as follows: For thin-film preparation, the specimens were deposited on freshly cleaved mica from boiling 0.1 wt % solutions in toluene. After evaporation of the solvent, the resulting films were melted and recrystallized at the desired temperatures, shadowed with Pt/C, coated with carbon, floated off the substrates onto water, transferred to Cu grids, and examined in a JEOL 100-CX transmission electron microscope at 100 keV. For single-crystal growth, the copolymers were dissolved in toluene to a concentration of 0.01 wt %. After crystallization at the desired temperatures, the crystal suspensions were deposited on mica. Following evaporation of the solvent, the procedure was the same as described for the preparation of the thin film specimens.

Results and Discussion

X-ray Diffraction. The X-ray diffractograms of the E–V copolymers and PE (fully reduced PVC) are presented in Figure 1. The room-temperature crystalline samples were obtained by quenching from the melt to ambient (only the copolymer E–V-37.3, with the highest chlorine content, was crystallized and recorded at 0 °C because it melts near room temperature). Compared with PE, the spacings of the main reflections, 110 and 200 of the orthorhombic unit cell, begin to appear at smaller angles as the chlorine content increases. For E-V-13.6 the 200 reflection appears only as a shoulder, and at higher chlorine content only the 110 reflection can be observed. This single peak has been indexed in a pseudohexagonal unit cell. Table II summarizes the most important structural features observed for the E–V copolymers. It is clear from these data that with increasing chlorine content a significant (~20%) expansion of the unit-cell

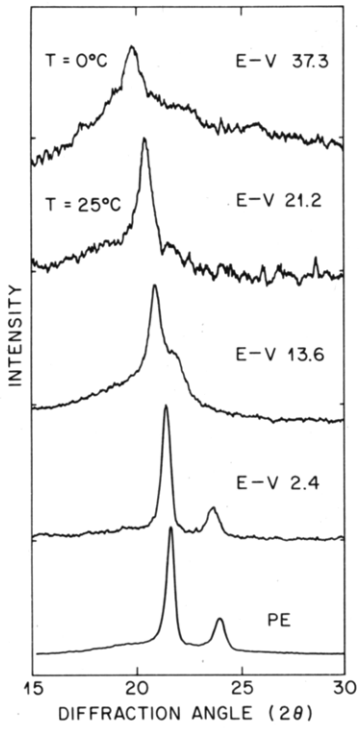

Figure 1. X-ray diffractograms for E–V copolymers and PE. All diffractograms were recorded at 25 °C except for E–V-37.3 at 0 °C.

basal plane is observed, mainly in the *a* direction. This is consistent with incorporation of the chlorine atoms into the crystal. As the proportion of V units increases, the unit cell expands indicating a substantial number of "defects" (Cl) trapped inside the crystal. This is also manifested by the increasing intermolecular disorder observed for the E–V copolymers with higher V contents, whose chains have an irregular cross-sectional profile and tend to pack like cylinders in a pseudohexagonal lattice. In light of their large crystallite thicknesses (see morphology section), these large effects cannot be explained solely by the structural strain produced by concentrating the V comonomer units in amorphous regions adjacent to the crystals. The above results are consistent with earlier studies demonstrating unit-cell expansion (primarily in the *a* direction) for other polyethylenes, e.g. those containing short[3] (methyl) or long[15] (butyl) branches as well as chlorinated[16] or brominated[34] ones. Moreover, they are in agreement with these and other[17] studies in supporting incorporation of Cl within the crystal lattice.

Table II
X-ray Structure of E–V Copolymers

polymer	d_{200}, Å	d_{110}, Å	*a*, Å	*b*, Å	system
PE	3.74	4.13	7.48	4.96	orthorhombic
EV-2.4	3.78	4.16	7.56	4.98	orthorhombic
EV-13.6	4.08	4.25	8.16	5.0	orthorhombic
EV-21.2	4.33	4.33	8.66	5.0	orthorhombic (pseudohexagonal)
EV-37.3	4.48	4.48	8.95	5.1	orthorhombic (pseudohexagonal)

Information concerning the conformation of the crystalline copolymer chains was obtained from X-ray fiber patterns of uniaxially oriented specimens. Figure 2 presents photographs for two E–V samples. The measured fiber period for all the copolymers is the same as that reported for PE. Therefore, no measurable change occurs in the *c*-axis dimension, indicating a retention of the planar zigzag, all-trans chain conformation.

The influence of V unit content on intermolecular crystal perfection can be estimated from the integral widths of the *hk*0 reflections in Figure 1 (after subtraction of instrumental broadening) by use of the Scherrer equation. Crystallite-size estimates are thus meant to incorporate distortion effects. Separation of size from distortion effects requires[35] the presence of multiple orders of reflection (ideally three or more) and therefore cannot be attempted for these copolymers. The average crystallite-size estimates of Figure 3 are seen to decrease with increasing chlorine content, though an asymptotic value is not necessarily implied. This indicates the highly defective character of the crystals formed in E–V copolymers with high V contents (large amount of chlorine incorporation). The values obtained for our samples are somewhat lower than those found in a comparable manner for polyethylene containing ethyl or longer branches[36] and remain so when plotted as a function of degree of crystallinity. This is consistent with enhanced incorporation of Cl into the lattice, leading to increased extents of defects and distortions.

Estimated crystallinities for the E–V copolymers as obtained from their X-ray diffractograms are presented in Figure 4 for specimens that had been quenched from

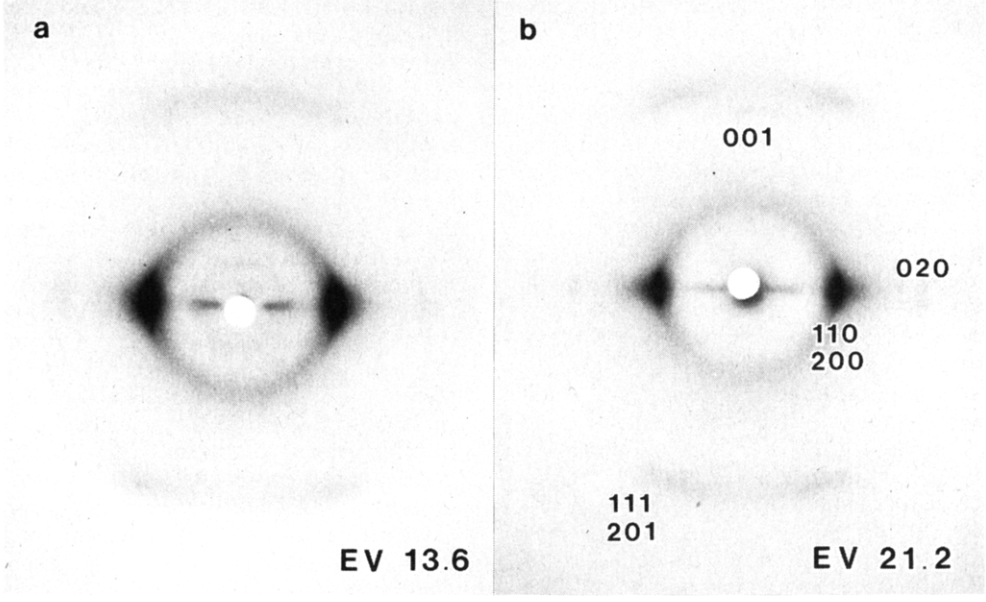

Figure 2. X-ray fiber patterns for uniaxially oriented specimens of E-V-13.6 (a) and E–V-21.2 (b).

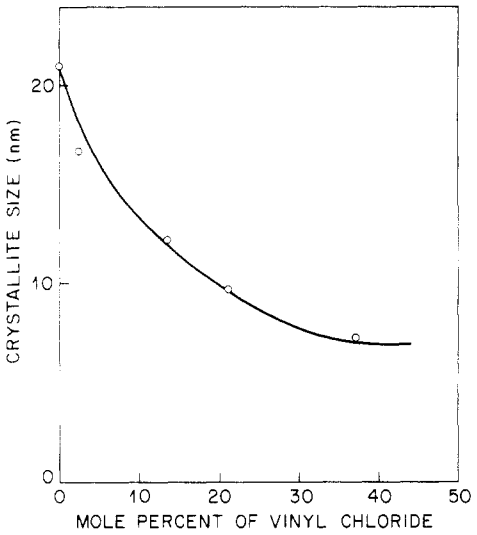

Figure 3. Estimated average intermolecular crystallite sizes in E–V copolymers obtained by X-ray diffraction.

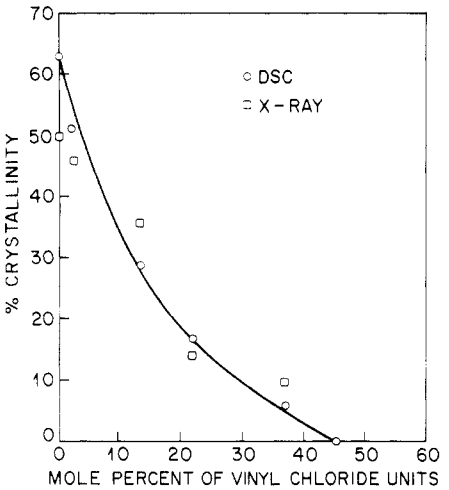

Figure 4. Comparison of the crystallinities of E–V copolymers as obtained by X-ray diffraction and DSC.

the melt to room temperature. Crystallinities derived from the enthalpies of fusion for the same samples are also shown in this figure. The observed trends are similar to those found for other ethylene copolymers.[12,36] We find no consistent differences in the crystallinities we determined by thermal or X-ray methods (see Figure 4). This is in agreement with Clas et al.,[36] who found such differences only for crystallinities exceeding 50%. Increasing chlorine content leads to rapid reductions in the crystallinity of E–V copolymers. This is also consistent with the incorporation of V comonomer units in the crystal. At low levels of V units, isolated Cl atoms may be easily incorporated into the crystal as point defects without causing further crystallographic damage. As the V unit content increases, the number of Cl's incorporated also increases, thus producing defective crystals with lower enthalpies of fusion and smaller crystallinities. Because crystallinities determined by thermal and X-ray methods are comparable, the amounts of heat required to melt a gram of PE and a gram of E–V crystals must be similar despite the structural defects observed in the E–V crystals. In addition, at higher Cl contents, because of the irregular distribution of a large number of the comonomer units, the number of uninterrupted, all-E unit sequences that may crystallize also decreases. For V unit contents above 40 mol %, the E–V copolymers can no longer be crystallized at all.[22]

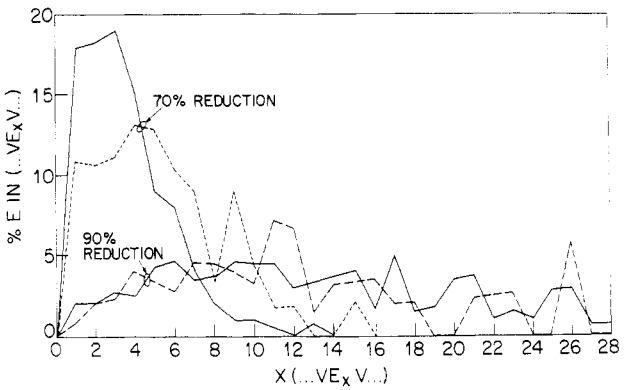

Figure 5. Percentage of E units in uninterrupted, all-E unit runs as a function of run length x and degree of reduction. Solid lines correspond to computer simulation of PVC reduction with $(n\text{-Bu})_3$SnH and dotted lines to the simulated results assuming random Cl removal.[27]

In Figure 5 we present the percentages of E units in our E–V copolymers that are found in uninterrupted, all-E unit runs as a function of the length of each run and the overall degree of $(n\text{-Bu})_3$SnH reduction, where 70 and 90% reductions correspond to E–V-30 and E–V-10 coplymers, respectively. These data were obtained in two ways:[27] (i) computer simulation of the $(n\text{-Bu})_3$SnH reduction of PVC and (ii) assuming the random removal of Cl during the reduction. These simulated data make clear that both the numbers and lengths of all-E unit runs in E–V copolymers obtained from the reduction of PVC with $(n\text{-Bu})_3$SnH are significantly reduced compared to those resulting from random Cl removal. Although not shown in Figure 5, for E–V-10 the percentage of E units in all-E unit runs ··· VE_xV··· with $x \geq 29$ is 27% for random Cl removal but just 14% for the $(n\text{-Bu})_3$SnH-reduced PVC. These observations help to distinguish our specimens from those examined previously in the literature and should be considered when the crystalline morphology of E–V copolymers obtained by the reduction of PVC with $(n\text{-Bu})_3$SnH is discussed.

Finally, other crystallization conditions have been employed to determine their effects on the structure and crystallinity of the E–V samples. For high chlorine content (>13.6 mol % V units), isothermal crystallization from the melt, or annealing of quenched samples at 5–20 °C below their melting points, gave the same expansions of the unit cell and similar degrees of crystallinity as those already reported for samples quenched from the melt. In the case of E–V-2.4, samples quenched from the melt and then annealed at temperatures 5–20 °C below its melting point showed a ca. 4% increase in crystallinity without significant variations in the unit-cell dimensions. This increase in crystallinity is consistent with other experimental evidence[15] and with expectations from the kinetic theory of Helfand and Lauritzen.[7] However, for our E–V copolymers with high V unit content, the amount of Cl trapped inside the crystal during growth appears to be independent of the conditions under which the copolymer was crystallized.

The independence of the crystallinity observed in our high-V copolymers from their thermal treatments is in contrast to that observed for ethylene copolymers whose co-units are not incorporated into the crystalline lattice. For these copolymers, slowly cooled samples show crystallinities significantly greater than those observed for quenched samples. The difference in the thermal behavior exhibited by our E–V copolymers is likely a result of their unique comonomer sequence distribution and may also explain why their crystalline microstructures are not

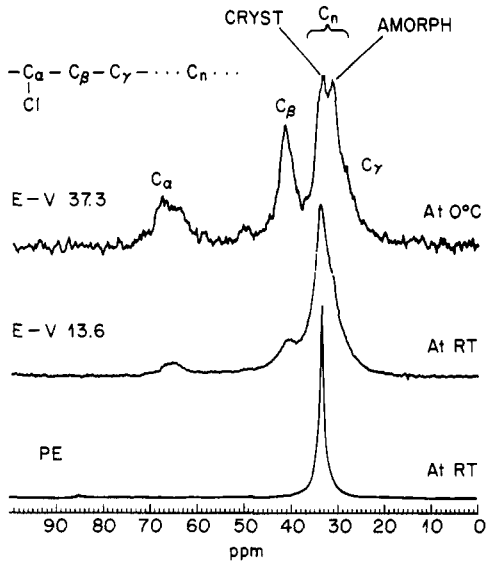

Figure 6. CPMAS/DD ^{13}C NMR spectra for two E–V copolymers and PE all quenched to room temperature from their melts.

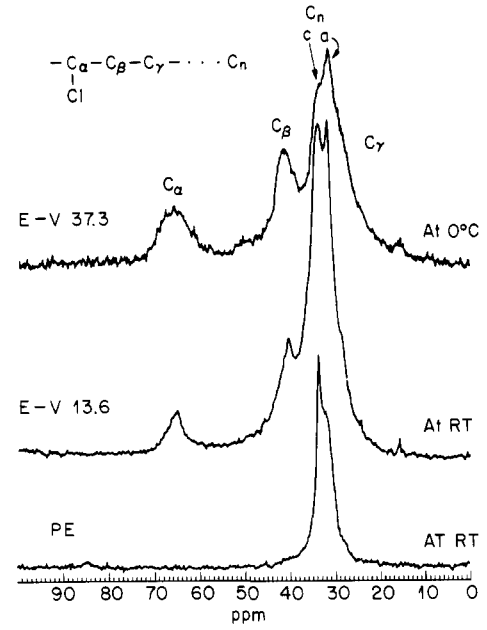

Figure 7. Same as Figure 6, but without cross-polarization.

governed by the Helfand–Lauritzen[7] theory of copolymer crystallization. As noted previously, the distribution of Cl's in our E–V copolymers is more nearly alternating than random and produces uninterrupted all-E unit runs that are shorter and fewer in number than from a completely random Cl distribution. Consequently, this microstructure is expected to reduce the effectiveness of annealing to produce larger, more perfectly ordered crystals because the extensive Cl distribution in the E–V copolymers prevents the formation of crystals without some incorporation of Cl atoms.

Solid-State ^{13}C NMR. Solid-state ^{13}C NMR with variable temperature control has also been used to study the structures of E–V copolymers. Figure 6 presents the cross-polarized (CP) spectra recorded with high power ^1H dipolar decoupling (DD) and rapid magic angle sample spinning (MAS) for PE and several E–V copolymers. Each of these samples was quenched from the melt to room temperature. Figure 7 presents spectra for the same samples obtained under the same conditions as used in Figure 6 except without CP. In the copolymers the resonance at 33.4 ppm is assigned to the crystalline CH_2 carbons in the trans conformation and the resonance at 31 ppm to the amorphous CH_2 carbons by analogy with PE.[33] We observe only a very small difference (0.3 ppm) in the chemical shift positions between the crystalline CH_2 resonances for PE and the E–V copolymers. This strongly suggests that the crystalline CH_2's in the copolymers also reside in the all-trans conformation as pointed out previously by the X-ray results.

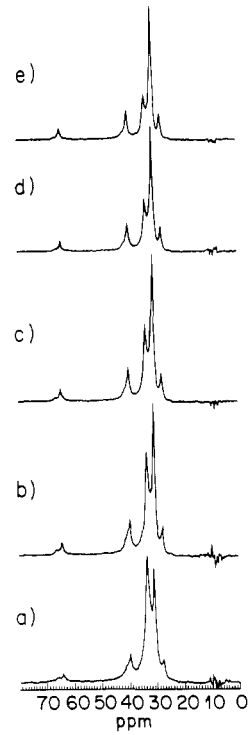

Figure 8. CPMAS/DD ^{13}C NMR spectra of E–V-13.6 recorded at 62 °C with different contact times: (a) 1.0, (b) 2.0, (c) 2.5, (d) 3.0, and (e) 3.5 ms.

As the Cl content increases, the amorphous CH_2 resonance also increases in intensity reflecting the decrease in copolymer crystallinity. For the copolymers with the highest Cl contents it is difficult to discriminate between the amorphous and crystalline resonances. Moreover, their spectra exhibit a significant upfield resonance. This behavior is most apparent in the copolymer spectra recorded without CP (Figure 7).

The copolymer spectra show several other resonances that are assigned to the carbons in the α-, β-, and γ-positions with respect to the chlorine substituent, by analogy to the spectra recorded in solution.[23] The peak centered at 65 ppm corresponds to the CHCl carbon and is ideal for monitoring the partitioning of Cl between the amorphous and crystalline phases. As observed in Figures 6 and 7, at room temperature it is difficult to determine the distribution of Cl between the phases because the CHCl resonance is broad, although in the spectrum without CP for E–V-13.6 the CHCl peak seems to narrow on its upfield side compared with the CP spectrum. However, by recording spectra at higher temperatures we have been able to resolve different CHCl resonances. We have taken advantage of differences in the proton, rotating-frame, spin–lattice relaxation times, $T_{1\rho}$ (^1H), to distinguish between the crystalline and amorphous CHCl resonances. Short contact times favor the observation of crystalline resonances while long contact times enhance the more mobile amorphous phase.[25]

Figure 8 presents a series of CP spectra obtained at 62 °C for E–V-13.6 by varying the contact times. This co-

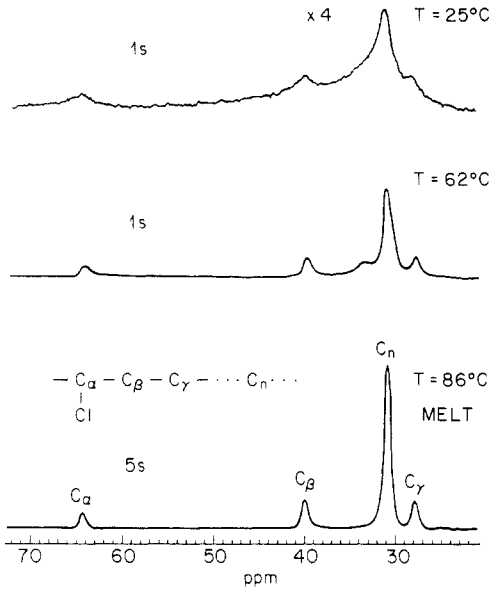

Figure 9. MAS/DD ^{13}C NMR spectra of E–V-13.6 recorded at (a) 25, (b) 62, and (c) 86 °C.

polymer melts at 78 °C, so at 62 °C it is still largely crystalline, but its amorphous phase is much more mobile than at room temperature (although at room temperature different contact times did indicate two phases for the CHCl carbon, the results are most apparent at high temperature where the amorphous carbons have the greatest mobility). In Figure 8b a sharp resonance at 64.8 ppm and a small shoulder at 66 ppm are observed for the CHCl carbon. These are assigned to the amorphous and crystalline phases of the sample, respectively, by comparison to the melt spectrum, where only a single CHCl resonance at 64.7 ppm is observed (see Figure 9). This assignment is confirmed by spin–lattice relaxation time measurements which show that the downfield resonance at 66 ppm has a T_1 three times longer than the more shielded resonance.

The β-CH_2 resonance exhibits a small downfield shoulder also ascribed to the crystalline phase. All of these results constitute clear experimental evidence for the inclusion of Cl inside the crystals of these semicrystalline E–V copolymers.

However, it is difficult to obtain quantitative information in a CP NMR experiment because of differences in the efficiency of CP for carbon nuclei in different phases.[19,37] Consequently, we resorted to an alternative set of experiments to get more detailed information concerning the distribution of Cl substituents between the crystalline and amorphous phases of E–V copolymers. Figure 9 presents the ^{13}C NMR spectra of E–V-13.6 obtained at different temperatures under DD and MAS, but without CP. Spectra were recorded with different delays in order to establish conditions under which only the amorphous carbons are observed. Previously the T_1 of each of the amorphous resonances was measured by the inversion–recovery method, and these data are presented in Table III. The spectrum at 86 °C (Figure 9c), where E–V-13.6 is in the melt, includes all of the carbons in the sample. The spectrum recorded at 62 °C, where the sample is still substantially crystalline, was obtained with a 1-s delay in order to observe only the amorphous carbons. The sample was quenched from the melt, and its spectrum was recorded at 62 °C under quantitative conditions, immediately following the observations made in the melt at 86 °C.

Intensity differences between both spectra give a measure of the amount of Cl included inside the crystals. The inner-CH_2 peak (C_n) shows a 35% loss of intensity compared with the total inner-CH_2 resonance (C_n) observed at 86 °C in the melt. This is in close agreement with the crystallinity measured for this sample by X-ray and DSC methods (see Figure 4). The CHCl resonance shows a 20% loss of intensity at 62 °C indicating at least 20% of the Cl's are included in the crystals. At 62 °C some partial melting occurs resulting in an increase in CHCl intensity and a decrease in our estimate of Cl incorporation. We have to point out that, although the spectrum recorded at 62 °C was acquired with a very short delay, a small portion of the inner CH_2 crystalline resonance at 33.4 ppm is still observed. Even though a similar observation is not detectable for the CHCl resonance, we nevertheless consider the 20% figure as a lower limit for the degree of Cl incorporation in the crystals.

Table III
^{13}C Spin–Lattice Relaxation Time, T_1, of the Amorphous Components[a]

samples	atom	T_1, s			
		T = 0 °C	T = 25 °C	T = 62 °C	T = 86 °C
polyethylene (PE)	CH_2		0.35		
E-V-13.6	CH_2 (PE like)	0.21	0.25	0.40	0.56
	$CH_2(\alpha)$		0.19	0.30	0.65
	$CH_2(\beta)$		0.18	0.23	0.37
	$CH_2(\gamma)$				0.43
E-V-37.3	CH_2 (PE like)	0.48	0.15		
	$CH_2(\alpha)$	0.97	0.20		
	$CH_2(\beta)$	0.61	0.11		
	$CH_2(\gamma)$				

[a] Measured by inversion recovery.[32]

Table IV
^{13}C Spin–Lattice Relaxation Time, T_1, of the Crystalline Components[a]

samples	atom	T_1, s		
		T = 25 °C	T = 62 °C	T = 86 °C
polyethylene	CH_2	50, 200	60	6
E-V-13.6	CH_2 (PE like)	7, 36	1	
	$CH(\alpha)$	6	1	
	$CH_2(\beta)$	11		

[a] Measured by Torchia[31] pulse sequence.

Structural information concerning the degree of disorder introduced inside the crystal by incorporation of Cl may also be provided by the dynamic NMR parameters. The T_1's measured for E–V-13.6 and PE at several temperatures are presented in Table IV. Both samples were crystallized under the same conditions (quenched from the melt) and have the same characteristics as noted in the Experimental Section. They differ only in their Cl content. It is observed that the copolymer has a much shorter T_1 for the crystalline, inner CH_2 carbons compared with PE, reflecting the disorder produced by inclusion of Cl substituents. As we observed by X-ray diffraction, incorporation of Cl into the crystal causes an expansion of the unit cell, and apparently this affects the motions of the lattice atoms, as detected by their T_1 values. There is also a significant decrease in the T_1's measured for both samples as the temperature is increased, indicating an increase in the thermally activated motion of their crystalline chains.

This important effect on the T_1 values produced by the incorporation of side chains was not observed in other crystalline ethylene copolymers by Axelson et al.[38] They found for a series of ethylene–1-alkene copolymers that the crystallite thicknesses and the interfacial structures were the most important characteristics of the semicrys-

talline state that controlled the T_1 values. An earlier study[39] demonstrated that the branching frequency and distribution affected primarily the T_1 values of the crystalline component. In comparing our T_1 values with those for other copolymers, we resort to the study by Axelson et al.,[38] who found that, irrespective of whether the side chains are included in the lattice or not, the T_1's are in the range of 40–50 s for ordered-sequence lengths (determined by Raman longitudinal acoustic mode) of ≤10 nm and for crystallinities < ca. 50%. For our 13.6 mol % copolymer, the crystallinity from Figure 4 is between 28 and 36% (depending upon experimental technique). The lamellar thickness (see our section on morphology) is ca. 20 nm, which in other ethylene copolymers[40] corresponds to ordered-sequence lengths of well under 10 nm. Therefore, on both of these counts our T_1 value of 36 s is close to expectation. This short T_1 may reflect slightly increased mobility of the crystalline segments as a result of Cl incorporation.

Finally, we should like to comment about the interfacial regions in our E–V copolymers. Until now we have considered the E–V copolymers to be organized in a simplified two-phase morphology (crystalline and amorphous) in order to interpret the NMR results in a straightforward fashion. But it is important to define the role of the interface in ethylene copolymers, as has been pointed out previously.[12,41] The NMR results permit us to conclude that *at least* 20% of the chlorine atoms are not in the truly amorphous phase. It is reasonable that some of these Cl's are at the interface, but certainly a significant portion are incorporated into the crystals and produce the large effects detected by X-ray (unit cell expansion) and NMR (reduction of T_1's for crystalline carbons). Our experimental evidence in support of the existence of an interphase in our E–V copolymers comes from the spin–lattice relaxation times observed for the crystalline component. As an example, for E–V-13.6 20% of the inner CH_2's in the crystal phase have a much shorter T_1 (7 s). In PE 10% of the crystalline signal also has a shorter T_1 (50 s). These shorter T_1 components in the inner CH_2 signals of PE and E–V have been reported by others.[19–21] These sequences still have an average trans conformation,[38,42] but with mobilities that are intermediate between the crystalline and amorphous carbons, and may thus represent interfacial material in our PE and E–V samples.

Our conclusion that the Cl's are primarily incorporated inside the crystals of E–V copolymers agrees qualitatively with observations made on several chlorinated polyethylenes (Cl-PE) by small-angle X-ray diffraction and neutron scattering.[16,17] Roe and Gieniewski[16] found the partition coefficient of Cl between crystalline and amorphous phases to be 0.15 and to decrease with the Cl content of the Cl-PE. On the other hand, Fischer et al.[17] found that Cl's were increasingly incorporated into the crystalline regions as the Cl content increased, until a random distribution of Cl between both phases was achieved. Our results agree more closely with those of Fischer et al. in the sense that there is a large Cl incorporation in the crystalline phase, which increases with E–V Cl content, although we have not observed a random Cl distribution between the amorphous and crystalline phases. The principal differences between these previous studies and ours are the methods used to prepare the samples (chlorination of PE vs dechlorination of PVC) and the Cl contents; in the previous studies the highest Cl content was 3 Cl/100 C (compare to Table I).

Morphology. In conjunction with our X-ray, thermal, and NMR studies of these copolymers, we have also investigated the effects of Cl incorporation on their morphology. Our discussion is centered primarily on specimens with the lower Cl contents, since the others have very low crystallinities. Nevertheless, we will present electron-microscopic and diffraction results for Cl contents up to 21.2 mol %, which exceeds by far the range of co-units covered in the literature (i.e., commonly up to 6 mol %).

Figure 10 (parts a and b) presents an electron micrograph and diffraction pattern of E–V-2.4 following isothermal crystallization at 95 °C. The crystals are seen to be clearly lamellar (the round regions represent remnants of the tributyltin hydride reducing agent used in the preparation of these copolymers, which is phase-separated). However, despite their lamellar habits, the crystals differ from those of PE in that their growth profiles are clearly rounded, with only rudimentary {110} facets being visible in some cases (arrows in Figure 10b). The corresponding electron-diffraction reflections (Figure 10a) are quite sharp, implying only very limited reduction of crystallinity, as was also shown by our X-ray and thermal results (Figure 4). The orientation of the electron-diffraction pattern with respect to the bright-field image shows that the *b* axis is the preferred growth direction of this copolymer, as is also the case for polyethylene.[43]

The spacings of the reflections in Figure 10a are only very slightly larger than those obtained by X-ray diffraction (Figure 1); such a slight lattice expansion resulting from the initial stages of radiation damage is common in electron diffraction of polymers. However, what is surprising is the intensities of the reflections in Figure 10a, which are clearly inconsistent with our X-ray data (Figure 1): we would have expected the diffraction pattern to be characterized by a very strong 110, an intermediate 200, and a weak 020 reflection. This is in fact observed when the sample is tilted around the *b* axis by 35° in only one direction (Figure 10c). This implies that the chain axes are inclined by 55° from the lamellar surfaces and that the latter are therefore the (201) (see schematic illustration in Figure 10e). Chain-axis tilting of this magnitude is well established for linear polyethylene[44–46] crystallized from the melt and has also been reported for single-crystal mats of branched polyethylene grown from solution.[47] While such a tilt is commonly invoked in other studies of ethylene copolymers (e.g. ref 12, 40), based upon results from linear PE, this is the first demonstration of the molecular inclination in individual melt-grown lamellae of ethylene copolymers. This tilt and the resulting (201) amorphous surfaces are well-known to arise from molecular crowding at the broad lamellar surfaces (e.g., ref 45), which is necessary to accommodate the density difference between chain segments in crystalline vs noncrystalline regions.[48]

Another important finding from Figure 10 is the fact that, even though many crystals contributed to the observed electron-diffraction pattern, the *hk*0 reflections were fully attained by tilting in only *one* direction (this despite the {110} faceting exhibited by some of these at their tips). We conclude that the molecular inclination is the same across and among all these crystals: The first implies that they are likely of the planar-sheet type,[45] rather than ridged or S-shaped, while the second implies some connectivity or common origin of these lamellae (e.g. through the agency of screw dislocations or overgrowths). It is also noteworthy that essentially the same morphology (i.e., curved lamellae with small {110} tips and unidirectional molecular tilt at ca. 55° across the full width of the crystal) has previously been reported[49] for polyethylene grown from dilute solution at high temperatures. All of these observations point to the structural and morphological similarity

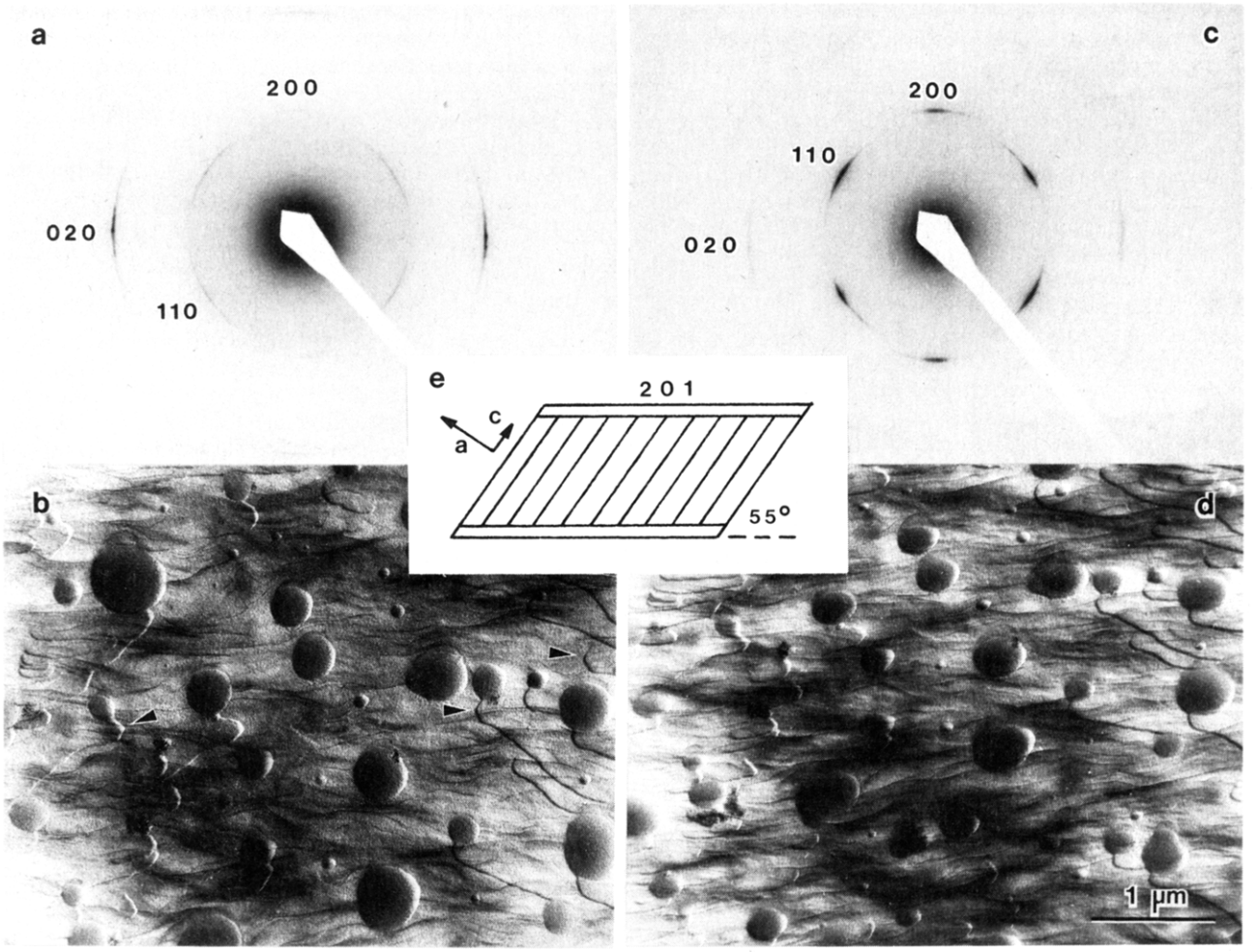

Figure 10. Electron micrographs and diffraction patterns of E–V-2.4 isothermally crystallized at 95 °C. Diffraction pattern (c) and micrograph (d) correspond to the same specimen as in (a, b), but tilted by 35° about the *b* axis. Inset (e) shows schematically the molecular inclination consistent with these diffraction patterns.

of our E–V-2.4 copolymer to linear polyethylene and strengthen our conclusion from X-ray and NMR techniques of significant Cl incorporation in the lattice without major crystallographic disruptions. We have also attempted to examine the presence or absence of molecular obliquity in crystals of higher Cl content but were unsuccessful because of their greatly reduced crystallite dimensions and order (see below).

The morphology of our E–V-2.4 copolymer crystallized at different temperatures is seen in Figure 11. In all cases, the characteristic habit is lamellar, but as expected those grown at the highest temperature are better developed and show somewhat more regular growth features (including faceting). In both isothermal-crystallization cases, the lamellae are quite long, exhibiting continuity over distances sometimes exceeding 10 μm. Those grown at the higher temperature have thicknesses (estimated from shadowing lengths) of ca. 24 nm, whereas those crystallized at 95 °C are somewhat thinner (ca. 20 nm). The latter are generally organized into spherulitic superstructures.

These morphologies may be compared with those of ethylene copolymers containing similar amounts (i.e., 2.2–2.7 mol %) of *ethyl* branches, which have been examined in detail by Voigt-Martin et al.[40] Samples slowly crystallized yielded lamellar morphologies which were of similar lengths and thicknesses as ours only for those whose sequence distributions were *not* random but favor sequential ordering of the comonomers. When the sequence distribution was more nearly random, the lamellae were significantly shorter and less regular.[40] The fact that our E–V copolymers show a greater regularity and continuity even though their sequence distribution is more toward the side of alternating, reflects the more facile and less distorting incorporation of Cl into the crystalline lattice.

The same conclusion may be reached by comparing specimens that had been quenched to ambient temperature. As seen from our Figure 11c, the E–V-2.4 copolymer still exhibits a distinctly lamellar morphology, even though the crystals are finer and shorter. Nevertheless, some lamellae are traceable to lengths of up to 1 μm. On the other hand, in the ethylene copolymers containing 2.2–2.7 mol % ethyl branches, immature lamellae that were highly segmented into very short crystallites were obtained *only* for copolymers with the more regular sequence distribution, whereas the more random-like had lost all lamellar character.[40] In examining our Figure 11c, we should also note that the lamellae in the rapidly cooled E–V-2.4 copolymer are organized with substantial mutual regularity. These are generally arranged in the form of spherulites, which moreover exhibit the banding characteristic of their polyethylene counterparts. In our case, the twist period is 0.5–0.6 μm, i.e. significantly smaller than in quenched polyethylene (1.0–1.2 μm). This may reflect a specific influence of the comonomer, e.g. through increased stresses resulting from lattice disorder or from increased concentration of defects at the lamellar surfaces.

The effects of higher Cl content on the morphology are examined in the following figures. Specifically, with Figure 12 we are already at a comonomer level (13.6 mol %) substantially exceeding the range that is normally studied.

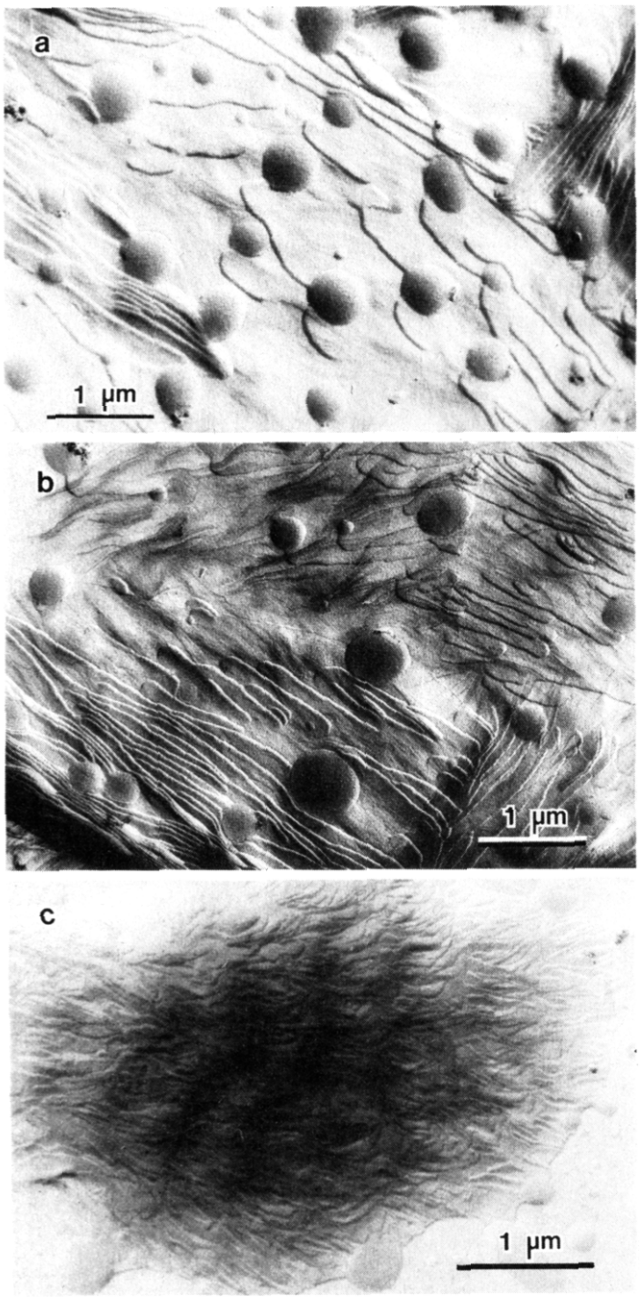

Figure 11. Electron micrographs of E–V-2.4 crystallized isothermally at (a) 103 °C and (b) 95 °C and (c) quenched to ambient temperature.

This range is generally up to 6 mol % (with the great majority of samples at the 0.2–4 mol % level) because of the very rapid and severe disorder imparted by most comonomers and/or branches. In the case of Cl, the morphological effects are seen to be milder presumably because of its smaller size and greater (and more uniform) incorporation in the crystals. As observed in Figure 12a, the E–V-13.6 copolymer crystallized at small undercoolings consists of lamellar crystallites, which are now much finer and shorter than for our 2.4 mol % samples (typical lengths are ca. 0.5 μm). Their widths are very narrow (they are difficult to determine exactly because of profuse overlaps) leading to fibrous-like crystals, in contrast to the broad ones seen in Figure 11. Nevertheless, such features are observed in other copolymers (e.g., ethyl-branched[40]) at much *lower* comonomer levels (typically 3–4 mol %). This signifies once again the relatively milder effect of Cl incorporation on the morphology of ethylene copolymers.

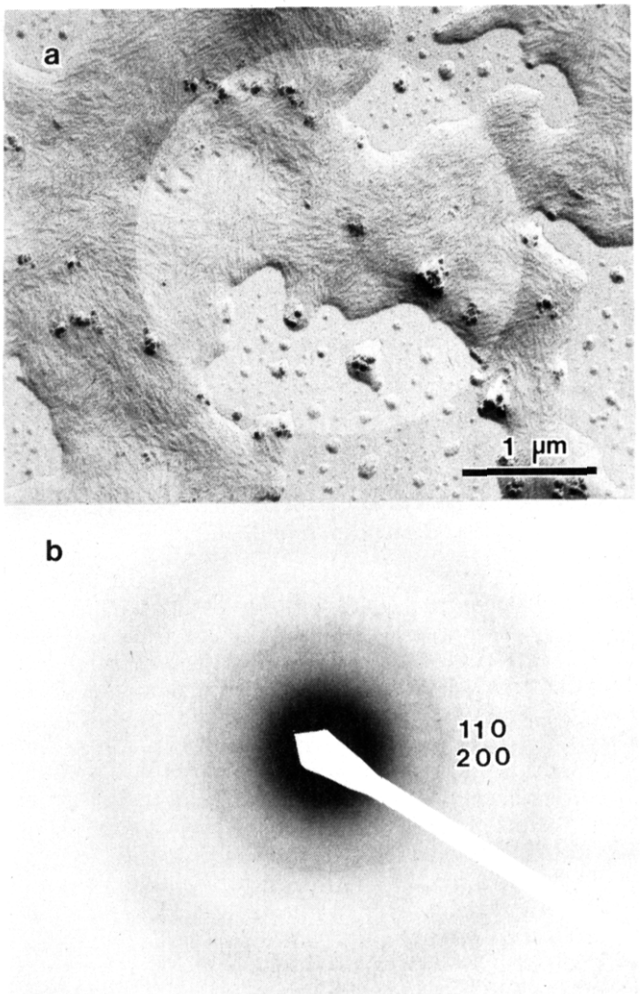

Figure 12. Electron micrograph (a) and diffraction pattern (b) of E–V-13.6 crystallized isothermally at 68 °C.

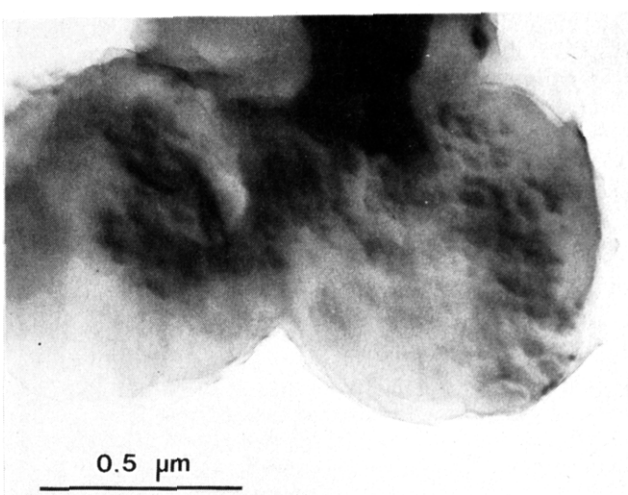

Figure 13. Electron micrograph of E–V-13.6 crystals grown by slow cooling of a dilute (0.01% w/v) solution in *n*-heptane to ambient temperature.

While discernible lamellae are formed in the 13.6 mol % copolymer, internal disorder is clearly evident in the corresponding electron diffraction pattern (Figure 12b) that shows considerable diffuseness in the (110, 200) reflection; its spacing is consistent with the unit-cell expansion seen in our X-ray diffractograms.

In an attempt to probe the limits of morphological regularity obtainable from this copolymer, we have crys-

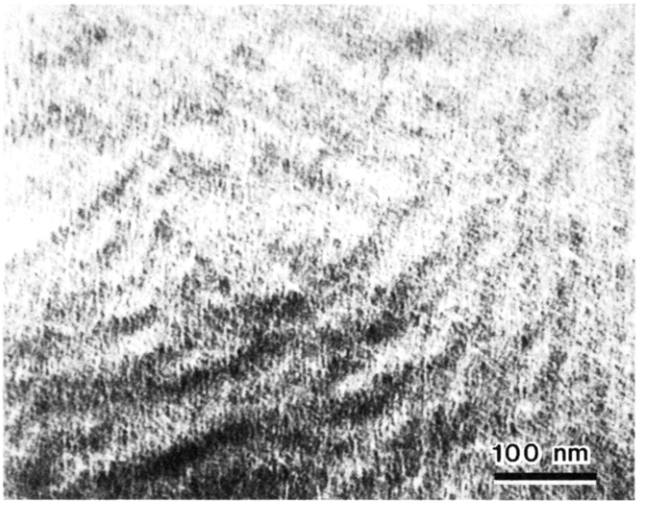

Figure 14. Electron micrograph of E–V-21.2 copolymer crystallized isothermally at 35 °C.

tallized it from dilute solution in *n*-heptane. Figure 13 shows typical morphologies. It is obvious that even under slow growth from such a dilute environment, there is no evidence of any crystallographic faceting or any regularity in habit. In this sense, our results are similar to those of Holdsworth and Keller,[47] who found loss of crystallographic faceting and substantial disordering (visible in increased arcing and broadening of reflections) in solution-grown single crystals of polyethylene containing ca. 5.6 mol % methyl branches. However, in that case the crystals were acicular and preserved the *b*-axis orientation of polyethylene. In our 13.6 mol % crystals, even these vestiges of morphological regularity are lost. The entities in Figure 13 are seen to be almost circular, to have very diffuse boundaries, and to be composed of much smaller (20–60 nm), irregularly shaped microcrystals. Electron diffraction also yields polycrystalline patterns. These results are broadly consistent with our X-ray and NMR findings and reflect morphologically the severe disorder inherent in these high-Cl chains.

Finally, we examine the morphological features of our 21.2 mol % copolymer crystallized from the melt (this is the sample of highest Cl content that has a melting point above room temperature). As is observed in Figure 14, this copolymer yields aggregates of short (<0.5 μm), curved, highly irregular lamellae that exhibit segmentation into much shorter microcrystallites. Their thicknesses are 25–30 nm, i.e. significantly larger than those of the other copolymers; because of the obvious morphological disorder, this increased thickness may arise primarily from the interfacial and amorphous regions as in alkyl-branched copolymers.[40] In general, we see that our E–V-21.2 copolymer behaves consistently with alkyl-branched ones of similarly low crystallinity (<15%), which, however, in the latter case occurs at much smaller comonomer contents.[36,40]

Conclusions

In summary, the present study of a series of ethylene–vinyl chloride copolymers with a sequence distribution on the alternating side of random indicates that a significant amount (>20%) of the Cl is incorporated inside their crystals. This conclusion was reached on the evidence provided by X-ray and electron diffraction, electron microscopy, and ^{13}C NMR techniques. The incorporation of Cl into the crystalline lattice causes progressive disordering of the structure and morphology of the E–V copolymers. Morphological characteristics of polyethylene, including *b*-axis growth and molecular inclination leading to (201) amorphous surfaces, have been confirmed for copolymers containing up to 2.4 mol % Cl. For higher Cl contents, or lower crystallization temperatures, the crystals become progressively more defective but retain a basically lamellar morphology.

References and Notes

(1) Flory, P. J. *Trans. Faraday Soc.* **1955**, *51*, 848.
(2) Swan, P. R. *J. Polym. Sci.* **1962**, *56*, 409.
(3) Baker, C. H.; Mandelkern, L. *Polymer* **1966**, *7*, 71.
(4) Cole, E. A.; Holmes, D. R. *J. Polym. Sci.* **1960**, *46*, 147.
(5) Shirayama, K.; Kita, S.; Watabe, H. *Makromol. Chem.* **1972**, *151*, 97.
(6) Vonk, C. G. *J. Polym. Sci., Part C* **1972**, *38*, 429.
(7) Helfand, E.; Lauritzen, J. I. *Macromolecules* **1973**, *6*, 631.
(8) Balta Calleja, F. J.; Hosemann, R. J. *J. Polym. Sci., Polym. Phys. Ed.* **1980**, *18*, 1159.
(9) Vonk, C. G.; Pijpers, A. P. *J. Polym. Sci., Polym. Phys. Ed.* **1985**, *23*, 2517.
(10) Landes, B. G.; Harrison, I. R. *Polymer* **1987**, *28*, 911.
(11) Killian, H. G. *Colloid Polym. Sci.* **1984**, *262*, 374.
(12) Alamo, R.; Domszy, R.; Mandelkern, L. *J. Phys. Chem.* **1984**, *88*, 6587.
(13) Richardson, M. J.; Flory, P. J.; Jackson, J. B. *Polymer* **1963**, *4*, 221.
(14) Bunn, C. W. In *Polyethylene*; Renfew, A., Morgan, P., Eds.; Illife: London, 1957; Chapter 5.
(15) Sanchez Cuesta, M.; Martinez Salazar, J.; Balta Calleja, F. J. *Polym. Bull.* **1987**, *17*, 23.
(16) Roe, R. J.; Gieniewski, C. *Macromolecules* **1972**, *6*, 212.
(17) Kalepky, U.; Fischer, E. W.; Herchenroder, P.; Schellen, J.; Lieser, G.; Wegner, G. *J. Polym. Sci., Polym. Phys. Ed.* **1979**, *17*, 2117.
(18) Laupetre, F.; Monnerie, L.; Barthelemy, L.; Vairon, J. P.; Sauzeau, A.; Roussel, D. *Polym. Bull.* **1986**, *15*, 159.
(19) VanderHart, D. L.; Perez, E. *Macromolecules* **1986**, *19*, 1902.
(20) Perez, E.; VanderHart, D. L.; Crist, B., Jr.; Howard, P. R. *Macromolecules* **1987**, *20*, 78.
(21) Perez, E.; VanderHart, D. L. *J. Polym. Sci., Polym. Phys. Ed.* **1987**, *25*, 1637.
(22) Bowmer, T. N.; Tonelli, A. E. *Polymer* **1985**, *26*, 1195.
(23) Schilling, F. C.; Valenciano, M.; Tonelli, A. E. *Macromolecules* **1985**, *18*, 356.
(24) Bowmer, T. N.; Tonelli, A. E. *J. Polym. Sci., Polym. Phys. Ed.* **1986**, *24*, 1631.
(25) Komoroski, R. A. *High Resolution NMR Spectroscopy of Synthetic Polymers in Bulk*; VCH: Deerfield Beach, FL, 1986.
(26) Jameison, F. A.; Schilling, F. C.; Tonelli, A. E. *Macromolecules* **1986**, *19*, 2168.
(27) Jameison, F. A.; Schilling, F. C.; Tonelli, A. E. *Chemical Reactions on Polymers*; Benham, J. L., Kinstle, J. F., Eds.; ACS Symposium Series 364; American Chemical Society: Washington, DC, 1988; Chapter 26.
(28) Starnes, W. H., Jr.; Schilling, F. C.; Plitz, I. M.; Cais, R. E.; Freed, D. J.; Hartless, R. C.; Bovey, F. A. *Macromolecules* **1983**, *16*, 790 and references cited therein.
(29) Mandelkern, L.; Stack, G. M.; Mathieu, P. J. M. *Anal. Calorim.* **1984**, *5*, 223.
(30) Flory, P. J.; Vrij, A. J. *J. Am. Chem. Soc.* **1963**, *85*, 3548.
(31) Torchia, D. A. *J. Magn. Reson.* **1978**, *30*, 613.
(32) Farrar, T. C.; Becker, E. D. *Pulse Fourier Transform NMR*; Academic Press: New York, 1971.
(33) Earl, W. L.; VanderHart, D. L. *J. Magn. Reson.* **1982**, *48*, 35.
(34) Landes, B. G.; Harrison, I. R. *Polymer* **1987**, *28*, 911.
(35) Buchanan, D. R.; Miller, R. L. *J. Appl. Phys.* **1966**, *37*, 4003.
(36) Clas, S. D.; Heyding, R. D.; McFaddin, D. C.; Russell, K. E.; Scammell-Bullock, M. V.; Kelusky, E. C.; St-Cyr, D. *J. Polym. Sci., Polym. Phys. Ed.* **1988**, *26*, 1271.
(37) Axelson, D. E., Chapter 5 in ref 25.
(38) Axelson, D. E.; Mandelkern, L.; Popli, R.; Mathieu, P. J. M. *J. Polym. Sci., Polym. Phys. Ed.* **1983**, *21*, 2319.
(39) Axelson, D. E. *J. Polym. Sci., Polym. Phys. Ed.* **1982**, *20*, 1427.
(40) Voigt-Martin, I. G.; Alamo, R.; Mandelkern, L. *J. Polym. Sci., Polym. Phys. Ed.* **1986**, *24*, 1283.
(41) Domszy, R. C.; Alamo, R.; Mathieu, P. J. M.; Mandelkern, L. *J. Polym. Sci., Polym. Phys. Ed.* **1984**, *22*, 1727.
(42) Kitamaru, R.; Horii, F.; Murayama, K. *Macromolecules* **1986**, *19*, 636.
(43) Keith, H. D. *J. Polym. Sci., Part A* **1964**, *2*, 4339.

(44) Keller, A.; Sawada, S. *Makromol. Chem.* **1964**, *74*, 190.
(45) Bassett, D. C.; Hodge, A. M. *Proc. R. Soc. London, Ser. A* **1981**, *A377*, 25.
(46) Stack, G.; Mandelkern, L.; Voigt-Martin, I. G. *Macromolecules* **1984**, *17*, 321.
(47) Holdsworth, P. J.; Keller, A. *J. Polym. Sci., Polym. Phys. Ed.* **1968**, *2*, 707.
(48) Frank, F. C. *Growth and Perfection of Crystals*; Doremus, R. H., Roberts, B. W., Turnbull, D., Eds.; Wiley: New York, 1958; p 529.
(49) Khoury, F.; Bolz, L. H. *Proc.—Annu. Meeting, Electron Microsc. Soc. Am.* **1980**, *38*, 242.

Conformation Aspect of Poly(γ-oleyl L-glutamate) with Long Flexible Side Chains As Studied by Variable-Temperature ^{13}C CP/MAS NMR Spectroscopy

Baijayantimala Mohanty,[†,§] Tadashi Komoto,[†,⊥] Junji Watanabe,[†] Isao Ando,[*,†] and Toru Shiibashi[‡]

Department of Polymer Chemistry, Tokyo Institute of Technology, Ookayama, Meguro-ku, Tokyo, Japan 152, and Tokyo Research Laboratory, Japan Synthetic Rubber Co., Ltd., Higashi-Yurigaoka, Asao-ku, Kawasaki, Japan. *Received August 22, 1988; Revised Manuscript Received March 29, 1989*

ABSTRACT: ^{13}C CP/MAS NMR experiments are carried out for poly(γ-oleyl L-glutamate) with unsaturated long side chains, as a function of temperature, in order to elucidate conformational features in the liquid-crystalline state. The experimental results show that the main chain of the polymer takes a right-handed α-helical conformation within the temperature range from −40 to 80 °C, while the long side chains are in a mobile state above −40 °C.

Introduction

It has been demonstrated that for a series of α-helical poly(L-glutamate)s with *n*-alkyl side chains of various lengths (where *n* is the number of carbon atoms in the alkyl group = 4–18), *n*-alkyl side chains longer than *n* = 10 form a crystalline phase composed of paraffin-like crystallites together with the α-helical main-chain packing into a characteristic structure.[1] The polymers form thermotropic cholesteric liquid crystals by melting of the side-chain crystallites. In order to obtain detailed information about the structure and dynamics of these cholesteric liquid crystals, it is very essential to study the structures and motion of the main chains and side chains at various temperatures.

Most recently, high-resolution CP/MAS (cross polarization/magic angle spinning) NMR, which is powerful tool for the structural and dynamic analyses of polymers in the solid state,[2-5] has been successfully applied to the investigation of the main-chain and side-chain structures and molecular motion in poly(L-glutamate) with *n*-alkyl side chains (*n* = 18) at room temperature[6] and also at other temperatures[7] through the observation of ^{13}C NMR chemical shifts in the solid state. The data show that the main chain of poly(γ-*n*-alkyl L-glutamate) assumes a right-handed α-helical conformation irrespective of the variable side-chain length and the *n*-alkyl chains assume an all-trans zigzag conformation.[6,7] These studies show that variable-temperature (VT) ^{13}C CP/MAS NMR experiments have the potential to provide detailed insight into the molecular structure and dynamics of these polymers in the solid and liquid-crystalline states.

As a continuation of these investigations, the purpose of this work is to investigate the structure of poly(γ-oleyl L-glutamate) (POLLG) with unsaturated side chains (*n* = 18) in the liquid-crystalline state as a function of temperature. The transition temperature between the solid and liquid-crystalline states of poly(γ-*n*-octadecyl L-glutamate) (*n* = 18) (POLG) is about 60 °C. But in the present case, DSC measurement clearly indicates that the crystallization of the side chains in POLLG does not occur over the temperature range from −40 to 80 °C. Thus, the polymer is in the liquid-crystalline state over a wide range of temperatures compared with POLG, even though the side chains of both the polymers have the same number of carbons. We attempt to elucidate the conformational behavior of both the side chains and the main chains as a function of temperature through the use of VT ^{13}C CP/MAS NMR experiments.

Experimental Section

Materials. Poly(γ-oleyl L-glutamate) was synthesized by ester-exchange reactions between poly(γ-methyl L-glutamate) (M_v = 100 000) and oleyl alcohol as described in a previous paper.[1] The complete replacement of methyl groups by oleyl groups was confirmed by ^1H NMR.

Measurements. ^{13}C CP/MAS NMR spectra were measured by means of a Bruker MSL-400 NMR spectrometer (100.6 MHz) with a VT CP/MAS accessory at temperatures form −40 to 80 °C. The sample (ca. 200 mg) was contained in a cylindrical rotor made of ceramic materials and spun at 3 kHz. Contact time is 2 ms and repetition time 5 s. Spectral width and data points are 27 kHz and 8K, respectively. The ^1H field strength was 2.0 mT for both the CP and decoupling processes. The number of accumulations was 160–200. ^{13}C chemical shifts were calibrated indirectly with reference to the higher field adamantane peak (29.5 ppm relative to tetramethylsilane ($(CH)_4Si$)). The field was calibrated at each temperature point used in the NMR experiments. The experimental error for the chemical shifts is within about ±0.1 ppm for the sharp peaks but more than ±0.1 ppm for the broad peaks as described below.

The DSC measurements were performed with a Perkin-Elmer DSC calorimeter. Wide-angle X-ray patterns were recorded with a flat-plate camera by using a Rigaku-Denki X-ray generater.

Results and Discussion

Thermal Behavior of Poly(γ-oleyl L-glutamate). We first compare the thermal behavior of POLLG with that

[†] Tokyo Institute of Technology.
[‡] Japan Synthetic Rubber Co., Ltd.
[§] Permanent address: Baijayantimala Mohanty, AT/PO Kortal, Jagatsinghpur, Dist-Cuttack, Orissa, India.
[⊥] Present address: Department of Polymer Chemistry, Gunma University, Tenjin-cho, Kiryu-shi, Gunma, Japan 376.

0024-9297/89/2222-4451$01.50/0